Available online at www.sciencedirect.com

SCIENCE DIRECT®

Coordination Chemistry Reviews 249 (2005) 299–311

COORDINATION CHEMISTRY REVIEWS

www.elsevier.com/locate/ccr

Review

A quantum chemical computational study of the relative stabilities of *cis*- and *trans*-platinum dichloride in aqueous solution

Noel S. Hush [a,b,*], Jens Schamberger [a,c], George B. Bacskay [a]

[a] *School of Chemistry, University of Sydney, Sydney, NSW 2006, Australia*
[b] *Department of Biochemistry, University of Sydney, Sydney, NSW 2006, Australia*
[c] *Graffinity Pharmaceuticals AG, Im Neuenheimer Feld 518-519, 69120 Heidelberg, Germany*

Received 23 December 2003; accepted 7 May 2004
Available online 22 July 2004

Contents

Abstract 299
1. Introduction 299
2. Computational methods 301
3. Gas-phase geometries and energetics of $PtCl_2(H_2O)_2$ 301
4. $PtCl_2(H_2O)_2$: solvation by application of a polarizable continuum model (COSMO) 304
5. $PtCl_2(H_2O)_2$: effective fragment potential approach to solvation 305
6. $PtCl_2(H_2O)_2$: solvation by combination of discrete and continuum methods 306
7. Conclusion 309
Acknowledgements 310
References 310

Abstract

Theoretical discussion of inorganic reaction mechanisms includes the role of the solvent, requiring estimates of thermodynamics of solvation in reactant, product or transition states. These are often made without reference to a “benchmark” calculation for a relatively simple, well-characterized system, which could provide a stringent test of their reliability. A convenient test system for such a calculation is $Pt(Cl)_2(H_2O)_2$, the *cis* and *trans* forms of which in solution exist in equilibrium and thus the relevant experimental thermodynamics is known very precisely [Inorg. Chem. 28 (1989) 3366, and earlier papers]. This paper reports a quantum chemical determination of the relative thermodynamic stabilities of *cis*- and *trans*-$[Pt(Cl)_2(H_2O)_2]$ in aqueous solution by a range of methods and basis sets, concentrating largely on the role of solvation. The methods employed include density functional (DFT) and coupled cluster theories, the conductor-like screening model (COSMO) of solvation and the effective fragment potential (EFP) method. The basis sets range from double zeta to 6–31+G(2*df*,*p*) on the ligands and a multiply polarized basis on Pt, in combination with a relativistic effective core potential (ecp). In the gas phase at 0 K, the *trans* − *cis* energy difference computed by coupled cluster methods is $0.1\,\mathrm{kcal\,mol^{-1}}$. The analogous value at 298 K in aqueous solution, obtained by DFT (B3LYP) and COSMO, is $-0.8\,\mathrm{kcal\,mol^{-1}}$, which is in good agreement with the experimental value of $-0.1\,\mathrm{kcal\,mol^{-1}}$. Modelling solvation by a combination of discrete (quantum chemical) and continuum (COSMO) methods, whereby four H_2O molecules are explicitly accounted for, yielded a value of $-1.5 \pm 1.0\,\mathrm{kcal\,mol^{-1}}$. These calculations demonstrate that DFT and polarizable continuum methods (PCMs) with appropriate basis sets are capable of yielding relative thermodynamic stabilities in solution of near chemical accuracy.

Keywords: Platinum complexes; *cis–trans* isomerism; Discrete and continuum solvation models; DFT calculations

1. Introduction

The research interests of Henry Taube, to whom this issue of *Coordination Chemistry Reviews* is dedicated, have spanned an extraordinarily wide range of topics. These

---

* Corresponding author. Fax: +61 2 9351 3329.
E-mail addresses: hush_n@chem.usyd.edu.au (N.S. Hush), drjens.schamberger@nexgo.de (J. Schamberger), bacskay@chem.usyd.edu.au (G.B. Bacskay).

0010-8545/$ – see front matter © 2004 Elsevier B.V. All rights reserved.
doi:10.1016/j.ccr.2004.05.021

generally raise interesting and fundamental questions about structure in ground and excited states, and the detailed nature of reaction pathways. These theoretical issues frequently have strong overlaps with our interests and, over quite a long period, work from this laboratory has addressed a number of them. As Taube's work is concerned almost exclusively with processes in solution, this has involved, in addition to molecular structural calculations, estimates of the often critical solvent effects. These are of two kinds. The first is concerned with equilibrium solvation. One such area is that of properties of the remarkably stable η^2 transition metal complexes in which molecular hydrogen (for long thought to be substitution-'inert') functions as a ligand [1–6] and their thermodynamics of ligand exchange [7]. A second is protonation-induced paramagnetism in osmium complexes [8], and a third is the nature of the Catalytica [9] Pt-complex homogeneous catalysis of methane to methanol in remarkably efficient yield [10,11].

Solvation plays a decisive role in determining structure and reactivity in these systems, and the theoretical studies have thrown considerable light on its significance in these unusual phenomena. Taube has also studied experimentally in detail the spectroscopy (particularly of the charge-transfer or intervalence transfer types) of transition metal complexes in solution. Here, of course, for vertical transitions, the solvent is frozen into the same configuration in ground and excited states. The study of solvent effects accompanying electronic excitation has been studied extensively by Zeng, Reimers and Hush: the resulting ZRH method for calculation of such effects has been applied to ligands such as pyridine [12], pyrazine [13], pyrimidine [14–16], and pyridazine [17] the metal-to-ligand charge transfer excitations of pentammine Ru(II) complexed with pyridine [18,19] or pyrazine [20] and the photogeneration of H_2 from Fe(II) in water solution [21,22]. The applications of ZHR solvation theory to transition metal systems have been reviewed by Hush and Reimers [23,24].

The solvation process in such calculations has been approached theoretically by several methods. There has not been, however, an in-depth study of the relative accuracies of such estimates either of microscopic structure of a solvated species or of the related thermodynamics of solvation for an individual test case. Such a test case is provided by the complexes of formula $Pt(Cl)_2(H_2O)_2$, which co-exist in equilibrium in water solution in *cis* and *trans* forms. The thermodynamics of this equilibrium are known experimentally to high accuracy from the work of Elding and Gröning [25–27] which provide a convenient benchmark for theoretical estimates. With this in mind, we have undertaken a study of the relative thermodynamic stabilities of these isomers in gas phase and in aqueous solution using a current range of standard quantum chemical methods and basis sets, with particular emphasis on the role of solvation.

Most chemical reactions take place in condensed media, most often in liquid phase, particularly in aqueous solution. A reliable computational modelling of such processes, in addition to the need for reasonably high level quantum chemical computation of the geometries and energies of the appropriate species, including thermal corrections, also requires an adequate treatment of solvent effects. In this regard, the chemistry of transition metal complexes has proved to be particularly challenging to computational chemists. As many such compounds play an important role in industrial catalytic processes [9–11], the accurate description of their properties in solution, while not an easy task, is especially important for the understanding of the underlying reaction mechanisms, especially in light of the paucity of experimental data.

The solvation of transition metal complexes in water may be described in terms of a range of different types of interactions. First, if there are water molecules, viz. ligands, in the first coordination shell of the metal, the metal–water bonds are generally quite strong, with considerable covalent character, and such ligands will have a direct influence on the electronic structure of the metal and hence its binding to other ligands. Secondly, the transition metal complex will be surrounded by a second shell of water molecules which may be strongly hydrogen bonded to the ligands in the first coordination shell. These molecules may directly participate in reactions of the complex, e.g. through proton transfer or nucleophilic addition. Thirdly, there will be further (bulk) solvation by subsequent shells of molecules whose structure will increasingly resemble the bulk solvent, although a degree of long-range order may occur via the long-range polarization of the solvent by the complex. These long-range effects can have some bearing on the relative stabilities of isomeric species of a transition metal complexes, as found for example by Siegbahn and Crabtree [28] in their study of the solvation of *cis*- and *trans*-$[Pd(II)Cl_2(H_2O)_2]$.

In ab initio and density functional calculations, solvent effects are generally accounted for through various implementations of the reaction field approach, where the solute molecule is placed in a cavity within a polarizable dielectric continuum representing the solvent [29]. While such models are useful for the modelling of bulk solvation effects, they are inappropriate in the case of strong solute–solvent interactions. Thus, in general, the recommendation is that as many of the solvent's water molecules as computationally practical should be modelled as discrete molecules, but at least those in the first and second coordination shell. Combining discrete molecular cluster calculations with dielectric continuum treatments of long range interactions is clearly a sensible way of approaching the problem and such techniques are increasingly used in studies of solvation [30]. As the explicit inclusion of solvent molecules in ab initio or density functional calculations can rapidly become a costly process, such calculations are still limited in their scope. To counteract and effectively eliminate such problems Gordon and co-workers developed the effective fragment potential (EFP) method [31–37], where the solute–solvent and solvent–solvent interactions are calculated via the effective potentials of the solvent molecules. The latter consist of terms that represent electrostatic (in the form of distributed multipoles), polarization, exchange repulsion and charge transfer interactions. Recent applications of the EFP method include the characterization of the equilibrium structures of water clusters with up to pentamers [38], studies of the neutral and zwitterionic forms of glycine in aqueous solution [30,39], the aqueous solvation of sodium chloride [40], acetic and formic acids [41], NaOH, HCl and HF [42], solvation effects on electronic transitions [43], and the modeling of enzyme active sites [44]. The demonstrated successes of the method encouraged us to apply it to the study of solvent effects on the energetics of simple transition metal complexes.

As indicated above, the subject of the current case study is platinum dichloride, viz. $PtCl_2(H_2O)_2$. Elding and Gröning obtained experimental data on the equilibrium between *cis* and *trans* platinum dichloride in aqueous solution [25–27]. On the basis of the measured equilibrium constant of 1.2 at room temperature, the free energy difference of 0.1 kcal mol^{-1} was derived, in favour of the *trans* isomer. The task of this study is to use current techniques of computational quantum chemistry to calculate the relative thermodynamic stabilities, viz. free energy difference, of these isomers, in gas phase and in solution. This will provide (hopefully) reliable theoretical estimates of solvation energies for this system as well as allow us to make a critical evaluation of the accuracy and reliability of the methods used, which include the conductor-like screening model (COSMO) of Klamt et al. [45–47], the EFP technique of Gordon and co-workers [31–42] as well as a combination of discrete and continuum methods.

2. Computational methods

The calculations reported in this paper were performed using a range of different methods. The (gas-phase) equilibrium geometries, vibrational frequencies and relative energies of *cis*- and *trans*-$PtCl_2(H_2O)_2$, as well as several clusters of these with four and eight water molecules, were determined by the application of density functional theory (DFT) utilizing the B3LYP functional [48,49]. The performance of DFT for the reliable prediction of relative energies was examined by comparisons with two mainstream correlated wave function methods: Møller-Plesset second-order perturbation (MP2) theory and coupled cluster theory with singles, doubles and perturbative triples [CCSD(T)] [50]. The majority of computations employ the 6–31G(*d*), 6–31+G(*d*,*p*), 6–31G(2*df*,*p*) and 6–31+G(2*df*,*p*) Gaussian bases for Cl, O and H, while for Pt the Stuttgart–Dresden relativistic effective core potentials (ecp) and SDD valence basis of Stoll and co-workers [51] are used, whereby a [6*s*, 5*p*, 3*d*] contracted Gaussian basis is utilized to accommodate the 5*s*, 5*p*, 5*d* and 6*s* valence electrons. (The SDD basis for all other atoms is the Dunning–Huzinaga valence double-zeta basis set [52].) In the calculations, which employ the 2*df* polarization sets, the Pt basis set was also extended by the addition of a 3*fg* polarization set ($\zeta_f = 2.1$, 0.7, 0.25; $\zeta_g = 0.3$). These exponents were optimized via B3LYP computations on *trans*-$PtCl_2(H_2O)_2$.

The solvation of *cis*- and *trans*-$PtCl_2(H_2O)_2$ by small numbers (4–35) of discrete water molecules was first studied by the effective fragment potential method [30–36], where the solute–solvent and solvent–solvent interactions are incorporated into the molecular Hamiltonian of the solute and where the (perturbed) wave function of the latter is obtained via standard quantum chemical methods. The EFP calculations in this work were carried out at the Hartree–Fock (EFP-HF) and MP2 (EFP-MP2) levels of theory, using the SBKJC effective core potentials and split-valence basis sets that have been developed by Stevens et al. [53–55]. The EFP optimized equilibrium geometries of the clusters with four and eight water molecules in the second (and possibly third) coordination shells also served as starting geometries for the subsequent B3LYP optimizations. Long-range solvation effects were computed by application of the conductor-like screening model [45–47] with water as solvent.

The EFP and related SCF and MP2 calculations were carried out using the GAMESS (US) programs (10 January 2000 version) [56]. The DFT, MP2, CCSD(T) and COSMO computations on $PtCl_2(H_2O)_2$ and its four and eight water clusters were performed using the Gaussian98 [57] and Gaussian03 programs [58]. All computations were performed on DEC alpha 600/5/333 and COMPAQ XP1000/500 workstations of the Theoretical Chemistry group at the University of Sydney and on the COMPAQ AlphaServer SC system of the Australian Partnership for Advanced Computing National Facility at the National Supercomputing Centre, ANU, Canberra.

3. Gas-phase geometries and energetics of $PtCl_2(H_2O)_2$

The computed gas-phase structures of *cis*- and *trans*-$PtCl_2(H_2O)_2$ are shown in Fig. 1. The corresponding bond lengths and angles listed in Table 1. Both isomers have C_2 symmetry. In the *cis* isomer, the C_2 axis lies in the (∼square) plane of the heavy atoms, bisecting the Cl–Pt–Cl and O–Pt–O angles, while in the *trans* isomer it is perpendicular to the plane of heavy atoms. As indicated by the bond angles in Table 1, the arrangement of the heavy atoms is slightly puckered. The Pt–Cl bond is calculated to be slightly longer in the *trans* isomer, while the opposite trend is noted for the Pt-O distances. These trends are consistent with the higher *trans*-influence of chloride ligands relative to water, so that bonds *trans* to a Pt–Cl bond would be expected to be weaker [59]. The arrangement of the water molecules in each isomer is such that one hydrogen in a given water is near-planar with the heavy atoms, allowing a for relatively short $H\cdots Cl$ distance of 3.2–3.4 Å. This suggests that there is a degree of hydrogen bonding between the water and chloride ligands. The *trans* − *cis* energy differences, as computed by DFT with five different basis sets appear to show a reasonable

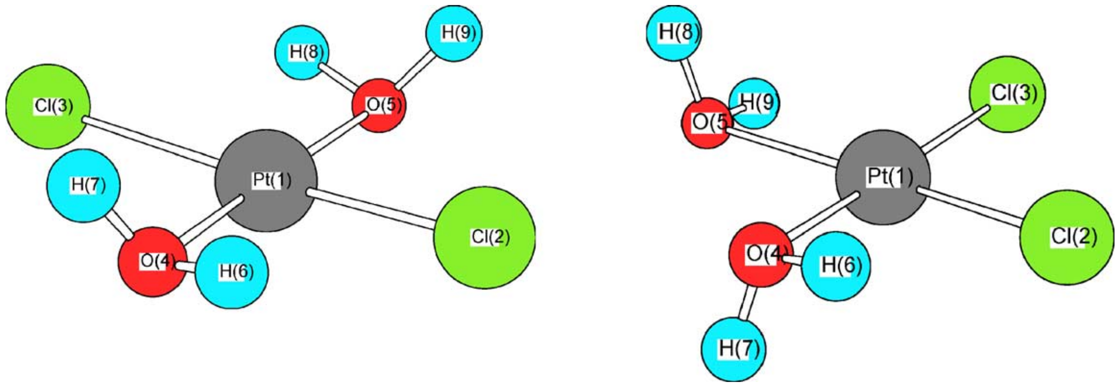

Fig. 1. Structures of *trans*- and *cis*-$PtCl_2(H_2O)_2$.

Table 1
trans- and *cis*-$PtCl_2(H_2O)_2$: computed equilibrium geometries at B3LYP/6–31G(*d*) level of theory

	trans	*cis*
R (Pt−Cl)	2.352	2.299
R (Pt−O)	2.072	2.158
R (O4−H6)	0.976	0.984
R (O4−H7)	0.976	0.975
α (Cl−Pt−Cl)	176.3	97.8
α (O−Pt−O)	178.2	95.1
α (O4−Pt−Cl2)	85.6	83.5
α (H−O−H)	108.2	105.3
τ (O4−Pt−Cl2−Cl3)	−91.0	180.0
τ (H6−O4−Pt−Cl3)	−165.5	10.1
τ (H7−O4−Pt−Cl3)	−50.6	−99.1
R (H6···Cl2)	2.55	2.46
R (H7···Cl3)	3.19	3.39[a]

Bond lengths in Å, bond and torsional angles in degrees (°).
[a] *R*(H7···Cl2).

degree of convergence. Polarization functions on the ligand heavy atoms are clearly of importance, while diffuse functions are less so. The comparison with CCSD(T) provides convincing evidence that DFT can reliably predict the *trans* − *cis* energy difference, i.e. within ~0.1 kcal mol^{-1}. By contrast, the performance of MP2 is less satisfactory: it differs from the CCSD(T) benchmark by 0.6 kcal mol^{-1}. In light of the demonstrated reliability of DFT, it was adopted as the method of choice for the computations on the larger clusters.

The net result of these calculations is that in the gas phase at 0 K the *trans* isomer is predicted to be marginally (by ~0.2 kcal mol^{-1}) more stable than the *cis* form. Inclusion of thermal contributions would lead to a free energy difference of just 0.06 kcal mol^{-1} at 298 K, with *cis* being the more stable isomer. These results closely match the experimental data of Elding and Gröning [25–27]. However, as the latter apply to the free energy difference in aqueous solution, the unexpected conclusion that emerges is that the solvation energies of the two isomers would also need to be essentially the same.

Burda et al. [60] have devised a Gaussian3 (G3) type theory for the study of platinum complexes, which also relies on the Stuttgart–Dresden ecp for Pt, but explicitly includes spin-orbit coupling and core-valence polarization effects. In the case of *cis*- and *trans*-$PtCl_2(H_2O)_2$, they find that the energetic contributions of each of these effects are quite similar in the two isomers. Their combined contribution to the *trans* − *cis* difference was computed to be 0.31 kcal mol^{-1}. Application of this correction to our CCSD(T)/6–31G(2*df,p*) energy difference yields a value of 0.11 kcal mol^{-1} as the free energy difference at 0 K. The corresponding G3 value of Burda et al. [60] is −0.19 kcal mol^{-1}, which agrees well with our results (Table 2).

Table 2
trans- and *cis*-$PtCl_2(H_2O)_2$: energy differences (including ZPE), free energies of solvation (computed by COSMO) and resulting free energy differences in aqueous solution at 0 K

Calculation	$\Delta E_0(trans - cis)$	$\Delta G_{solv}(trans)$	$\Delta G_{solv}(cis)$	$\Delta\Delta G_{solv}(trans - cis)$	$\Delta G_{aq}(trans - cis)$
B3LYP/SDD	−4.96	−20.35	−20.79	0.44	−4.52
B3LYP/6–31G(*d*)[a]	0.17	−22.68	−21.34	−1.34	−1.17
B3LYP/6-31 + G(*d,p*)[a]	−0.11[b]	−22.63	−21.34	−1.29	−1.41
B3LYP/6–31G(2*df,p*)[c]	−0.30[b]	−21.96	−21.45	−0.51	−0.80
MP2/6–31G(2*df,p*)[c]	0.41[b]				
CCSD(T)/6–31G(2*df,p*)[c]	−0.20[b]				
B3LYP/6–31+G(2*df,p*)[c]	−0.30[b]	−22.15	−21.13	−1.02	−1.33

All energies in kcal mol^{-1}.
[a] Pt basis: SDD.
[b] Geometry and ZPE computed at B3LYP/6–31G(*d*) level: $E_{ZPE}(trans) = 34.01$ kcal mol^{-1}, $E_{ZPE}(cis) = 33.76$ kcal mol^{-1}.
[c] Pt basis: SDD + 3*fg*.

Table 3
trans- and *cis*-$PtCl_2(H_2O)_2$: non-zero components of dipole (μ, in D) and quadrupole moments[a,b] (traceless, θ, in DÅ) and atomic charges[c] (q, in e) obtained by Roby–Davidson and NBO methods

Property	*trans*	*cis*
μ_z	2.50	6.64
θ_{xx}	18.78	−1.67
θ_{yy}	−16.21	4.62
θ_{zz}	−2.57	−2.95
θ_{xy}	−3.41	4.15
q(Pt)	0.40[d], 0.65[e]	0.26[d], 0.58[e]
q(Cl)	−0.27[d], −0.55[e]	−0.30[d], −0.44[e]
q(O)	−0.45[d], −0.86[e]	−0.35[d], −0.90[e]
q(H)	0.26[d], 0.54[e]	0.26[d], 0.53[e]

[a] The z-axis in the case of both isomers is the C_2 symmetry axis. In the *trans* isomer, the O and Cl atoms lie approximately on the x- and y-axes, respectively. In *cis* isomer the x-axis is perpendicular to the plane of heavy atoms, with z bisecting the OPtO and ClPtCl angles.

[b] B3LYP/6–31+G(2*df,p*).

[c] B3LYP/6–31G(*d*).

[d] Roby–Davidson atomic charges.

[e] NBO atomic charges.

The computed dipole and quadrupole moments of the two isomers are listed in Table 3, along with the results of population analyses, viz. atomic charges. As required by symmetry, in each isomer non-zero component of the dipole moment coincides with the C_2 symmetry axis. As one would expect, the *cis* isomer has a substantially larger dipole than the *trans* isomer. The reverse appears to hold, however, for the quadrupole moment.

The two sets of atomic charges, computed by two different approaches, viz. Roby–Davidson (RD) [61–64] and natural bond orbital (NBO) [65–67] methods are consistent with each other, although NBO predicts a higher degree of polarity, viz. larger positive and negative charges on the individual atoms than obtained by the RD method. The resulting polar nature of the bonds is of course consistent with the large dipole and quadrupole moments discussed above.

As a further aid to the understanding of bonding and interactions within each complex, we investigated the rigidity of the structures with respect to the torsion of the water ligands. Relaxed scans of the potential energy surfaces were generated for a range of torsional angles, whereby for each fixed value of the H6–O–Pt–Cl2 dihedral angle (see Fig. 1) the total energy (at the B3LYP/6–31G(*d*) level) was minimized with respect to all other geometric parameters. The resulting torsional potentials are shown in Fig. 2. If the geometries are constrained to maintain their C_2 symmetries, i.e. both water molecules are rotated in the same direction, the highest rotational barriers are calculated to be 11.8 and 4.6 kcal mol^{-1} for the *cis* and *trans* isomers, respectively. However, if the symmetry constraint is lifted, the barriers drop to about half these values, to 5.5 and 1.7 kcal mol^{-1}, respectively. Note that in the case of the *cis* isomer C_2 symmetry is maintained in the 0°–90° (and 270°–360°) region. These results suggest that the water ligands could display large amplitude internal rotation, especially in the *trans* isomer, where the torsional modes would be best described as hindered rotations.

These torsional potentials, to some extent at least, reflect the long-range electrostatic interactions of the ligands. For example, for the *cis* isomer the difference in water–water interactions between the equilibrium and the 180° structures (the latter corresponding to the highest rotation barrier) was estimated to be 3.7 kcal mol^{-1}. (This value was obtained by comparing the energies of two water dimers whose geometries are those assumed in the equilibrium and the 180° structures of the complex.) In the *cis* isomer, interactions with the Pt–Cl bond dipoles are also expected to be important. By

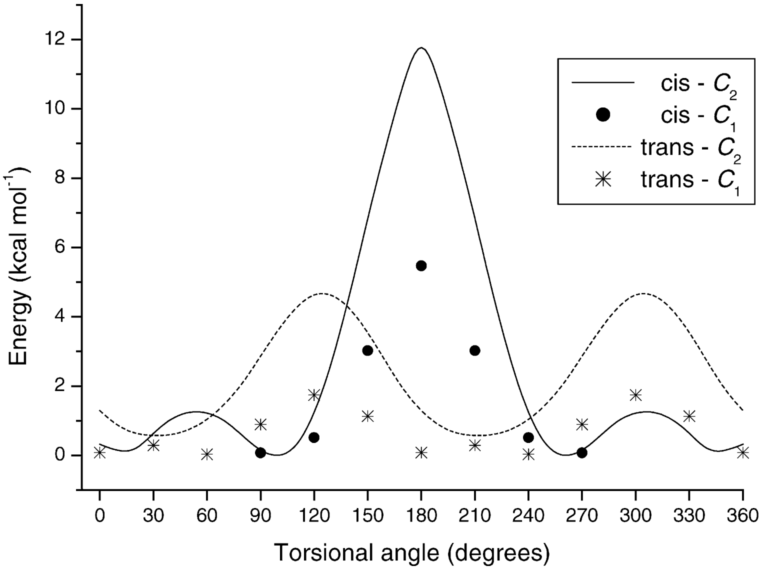

Fig. 2. *trans*- and *cis*-$PtCl_2(H_2O)_2$: torsional potentials with respect to H6–O–Pt–Cl2 dihedral angle in C_2 and C_1 symmetries computed at B3LYP/6–31G(*d*) level of theory.

contrast, in the *trans* isomer the dipole–dipole interactions among the water and Pt–Cl moieties would be less sensitive to the precise orientation of the water molecules, as would be the water–water interactions. The less hindered nature of the torsion in the *trans* isomer is also reflected in the low harmonic torsional frequencies of 84 and 127 cm^{-1}, to be compared with 206 and 234 cm^{-1} of the *cis*.

4. $PtCl_2(H_2O)_2$: solvation by application of a polarizable continuum model (COSMO)

Dielectric continuum methods represent a formally simple and popular approach to model solvation [29]. The simplest of these, the Born–Onsager approach, describes solute solvent interaction in terms of the solute's charge and dipole moment with the surrounding polarizable continuum representing the solvent. In the case of *cis*- and *trans*-$PtCl_2(H_2O)_2$, this model would predict a much larger solvation energy for the *cis* isomer, as its dipole moment (see Table 3) is ~2.5 times larger than for the *trans* isomer. Application of a generalised Born–Onsager type approach that includes quadrupole and higher multipole moments of $PtCl_2(H_2O)_2$, as in the self-consistent multipole moment reaction field (SCMMRF) theory [68], will redress the balance, given the high quadrupole moment of the *trans* isomer. A SCMMRF calculation utilising the multipole moments and dipole polarizabilities computed at the B3LYP/6–31G(*d*) predicts a *trans* − *cis* solvation energy difference of just 1.2 kcal mol^{-1}.

Polarizable continuum methods (PCMs), where the solute occupies a cavity whose geometry is determined by the shape, viz. charge distribution, of the solute molecule and where the solute–solvent interaction is determined via integration over the (virtual) charge distribution on the surface of the cavity [69] are superior to the Born–Onsager model and its variants. COSMO, in particular, represents an efficient and accurate implementation of PCM, hence it is the method of choice in this work.

The free energies of solvation computed by COSMO, using DFT with five different basis sets are listed in Table 2. The computed solvation energies are quite stable to basis set variations, once the basis includes polarization functions on the ligand heavy atoms. All such calculations (i.e. excluding B3LYP/SDD) predict the *trans* isomer to be slightly better solvated. The *trans* − *cis* difference in solvation energies ranges from −0.5 to −1.3 kcal mol^{-1}, while the differences in total free energies (at 0 K) range from −0.8 to −1.4 kcal mol^{-1}. Thermal corrections, as discussed above, would make a positive contribution of 0.26 kcal mol^{-1} to this quantity, while spin-orbit and core-valence polarization effects would add another 0.31 kcal mol^{-1}. The best estimate of the *trans* − *cis* free energy difference at 298 K, based on ΔG_{aq}[B3LYP/6–31+G(2*df*,*p*)] = −1.33 kcal mol^{-1} plus the above corrections, is then −0.76 kcal mol^{-1}. The agreement with the experimental value of −0.1 kcal mol^{-1} is

Table 4
Relative energies of *trans*- and *cis*-$PtCl_2(H_2O)_2 + nH_2O$ clusters and *trans* − *cis* energy differences calculated by the Effective Fragment Potential method at the HF/SBKJC level of quantum chemical theory

System	E(*trans*)	E(*cis*)	ΔE(*trans* − *cis*)	ΔE(mean)
$PtCl_2(H_2O)_2$	0.0	12.1	−12.1	−12.1
$PtCl_2(H_2O)_2 + 4H_2O$	−49.5	−39.0	−10.5, −14.6,	−12.4
	−49.4[a]	−34.9[a]	−14.5, −10.4	
$PtCl_2(H_2O)_2 + 6H_2O$	−66.1	−59.6	−6.6	−6.6
$PtCl_2(H_2O)_2 + 8H_2O$	−85.1[a]	−83.5[a]	−1.6, −1.1,	−0.8
	−84.1	−84.0	−0.1, −0.5	
$PtCl_2(H_2O)_2 + 10H_2O$	−103.5	−102.8	−0.8, 2.1, −0.3,	−1.8
	−106.0	−105.6	−3.3, −0.4, −2.8,	
	−107.6	−103.3	−4.9, −2.0, −4.4	
$PtCl_2(H_2O)_2 + 12H_2O$	−121.6	−118.2	−5.7, −6.9, 0.8,	−3.9
	−125.1	−119.4	−2.3, −3.5, 2.4,	
	−127.3	−124.0	−7.9, −9.1, −3.3	
$PtCl_2(H_2O)_2 + 14H_2O$	−139.6	−139.8	0.2, 2.0, 7.2,	−0.2
	−143.3	−141.6	−3.5, −1.7, 3.5,	
	−146.0	−146.8	−6.2, −4.4, 0.8	
$PtCl_2(H_2O)_2 + 16H_2O$	−170.1	−158.3	−12.6, −13.8, −11.3,	−6.8
	−170.9	−157.1	−11.8, −13.0, −10.5,	
	−189.4	−159.6	−12.9, −4.5, −9.2	
$PtCl_2(H_2O)_2 + 35H_2O$	−354.0	−356.2	2.2	2.2

All energies in kcal mol^{-1}.

[a] Symmetric structures.

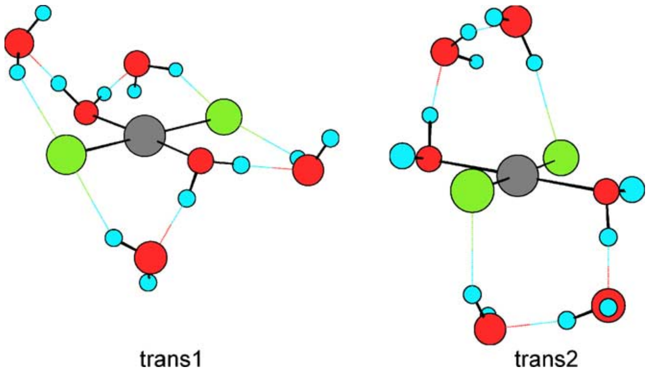

Fig. 3. Structures of [*trans*-$PtCl_2(H_2O)_2 + 4H_2O$] clusters.

excellent, although it might well be somewhat fortuitous. In the following sections, we will discuss the results of a discrete molecular approach to solvation.

5. $PtCl_2(H_2O)_2$: effective fragment potential approach to solvation

A series of EFP calculations at the Hartree–Fock level of theory were carried out for *cis*- and *trans*-$PtCl_2(H_2O)_2$ surrounded by a number (4–35) of water molecules (represented in terms of EFPs). The starting structures were obtained on the basis of molecular dynamics simulations (using the AMBER force field as implemented in Hyper Chem 5.0 [70] with TIP3P water potential) by systematically removing the furthermost water molecules. Thus, initially clusters with 35 solvating waters were generated, the geometries of which were then optimised by the EFP method. By removing more water molecules, a range of starting structures, with 16, 14, 12, ... solvent molecules, were obtained. The energies of a number of EFP optimised clusters are summarised in Table 4. The equilibrium structures of some hydrated clusters (subsequently re-optimized at the B3LYP/6–31G(*d*) level are shown Figs. 3–7, including those with the maximum number (35) of solvent molecules considered in this work.

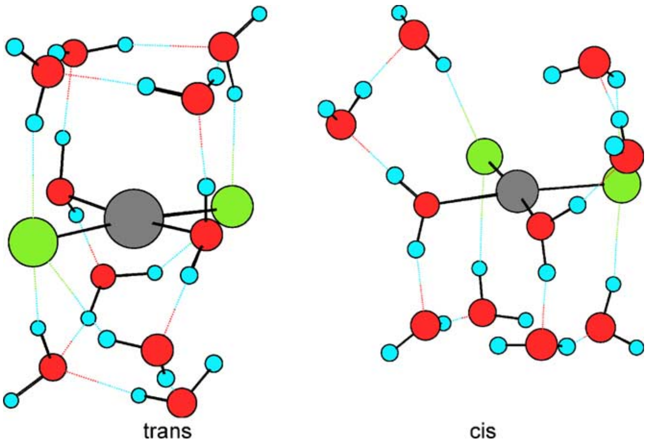

Fig. 5. Structures of [*trans*- and *cis*-$PtCl_2(H_2O)_2 + 8H_2O$] clusters.

Given the equilibrium structures of *cis*- and *trans*-$PtCl_2(H_2O)_2$, some degree of hydrogen bonding is expected to be present between the water and chloride ligands in both isomers. When solvated by four water molecules, the latter act as bridges between the water and chloride ligands, by forming hydrogen bonds with both. The two *trans* structures shown in Fig. 3 are qualitatively quite different, but their energies are effectively the same. In the case of the *cis*- + $4H_2O$ clusters (Fig. 4), the lowest energy isomers are a “symmetric” one (*cis*1) with four bridging waters linking the water and chloride ligands and two “asymmetric” ones (*cis*2 and *cis*3), which have bridges as well as a “dangling” chain of waters. With eight solvating water molecules it is possible to have highly “symmetric” structures where the four bridges between water and chloride ligands consist of two water molecules each, but also less symmetric structures, as shown in Fig. 5, with less regular bridges. The energies of the four $PtCl_2(H_2O)_2 + 8H_2O$ clusters are very close, suggesting that increased solvation favours the *cis* isomer. There appears to be a steady progression inasmuch as the *trans* − *cis* energy difference increases from $\sim -12\,\mathrm{kcal\,mol^{-1}}$ to $\sim -1\,\mathrm{kcal\,mol^{-1}}$, as the number of solvent molecules increases to eight.

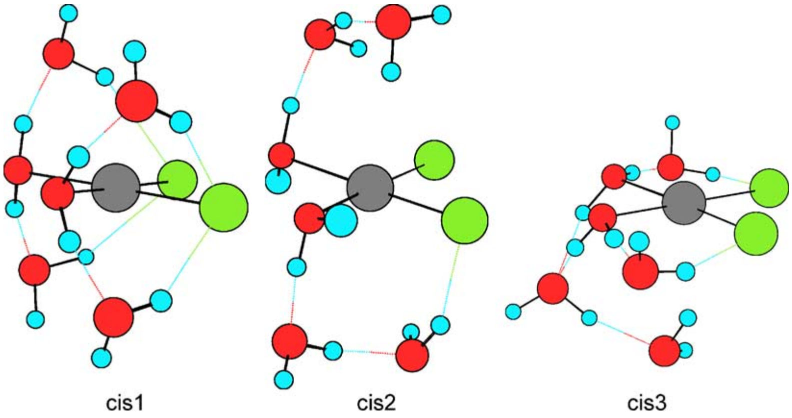

Fig. 4. Structures of [*cis*-$PtCl_2(H_2O)_2 + 4H_2O$] clusters.

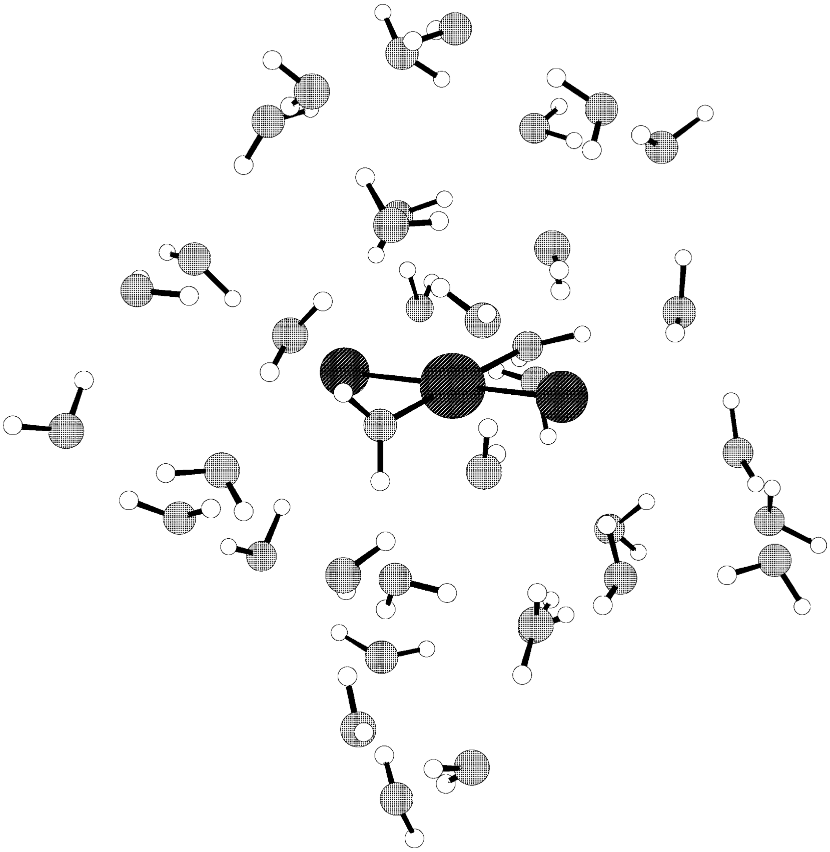

Fig. 6. Structures of [*trans*-$PtCl_2(H_2O)_2 + 35H_2O$] clusters.

However, as the results in Table 4 show, the *trans* − *cis* energy difference fluctuates markedly with a further increase in the number of solvent molecules. Moreover, the increasingly larger number of possible structures for each cluster, as the size of the cluster grows, makes these type of EFP calculations more and more computationally demanding without any apparent indication of convergence. A much larger number of configurations ought to be considered, as in Monte-Carlo or Molecular Dynamics (MD) simulations, to obtain statistically reliable results. We note that the recent versions of the GAMESS (US) programs have the capability of carrying out MD simulations where the interactions are described by the EFP model [71,72]. As much of our work, including all EFP calculations, were completed during 2000, i.e. prior to the release of these codes, we have not been able to utilize the newer methods offered by GAMESS.

The *trans* − *cis* energy difference for $PtCl_2(H_2O)_2$ and the symmetric four and eight water clusters was also computed by the EFP approach at the MP2 level. The results, included in Table 4, suggest that in EFP calculations the role of electron correlation is relatively minor but non-negligible. On the other hand, the EFP-HF *trans* − *cis* energy differences for these clusters were found to agree to within $1\,kcal\,mol^{-1}$ with the results of the analogous (supermolecule) Hartree–Fock calculations with the same basis, demonstrating the consistency and reliability of the EFP method. The basis set dependence of these results is addressed in the next section.

6. $PtCl_2(H_2O)_2$: solvation by combination of discrete and continuum methods

In light of the problems with discrete solvation models, as encountered in our EFP studies above, the combination of discrete and continuum methods of solvation, whereby the inner solvation shell(s) are included, as discrete molecules, in the quantum chemical treatment of the system, with long-range effects accounted for by a continuum method, might be regarded as the most reliable, chemically reasonable and computationally practical approach. In this final part of our study, several different equilibrium structures of *cis*- and *trans*-$PtCl_2(H_2O)_2$, explicitly hydrated by four and eight water molecules, were re-optimized at the B3LYP/6–31G(*d*) level, followed by single point B3LYP energy calculations with larger bases at the B3LYP/6–31G(*d*) equilibrium geometries, both in gas phase and in aqueous solution, using COSMO as the solvation model. The results are summarised in Tables 5 and 6.

In the case of the $PtCl_2(H_2O)_2 + 4H_2O$ clusters, two *trans* and three *cis* structures were used, as shown in Figs. 2 and 3. The relative gas-phase energies of the clusters, as shown

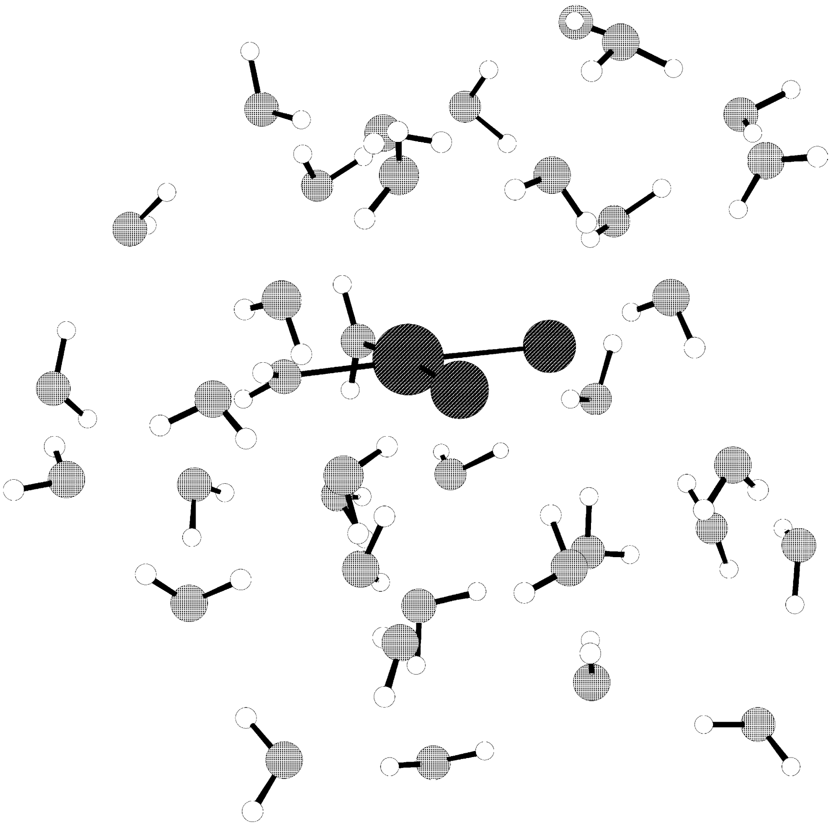

Fig. 7. Structures of [*cis*-$PtCl_2(H_2O)_2$ + $35H_2O$] clusters.

in Table 5, display a significantly greater degree of variation with basis than the parent complexes (see Table 2). This is due to the more stringent basis requirements associated with the quantum chemical characterization of hydrogen bonds. While the solvation energies, as computed by COSMO, are nearly a factor of two smaller in magnitude than for the parent systems, the fluctuation with basis is actually larger. The net result is that the free energies in solution also show

Table 5

trans- and *cis*-$PtCl_2(H_2O)_2$ + $4H_2O$ clusters: energy differences (including ZPE), free energies of solvation (as computed by COSMO) and resulting free energy differences in aqueous solution at 0 K

Calculation	X	$\Delta E_0(trans1-\mathrm{X})$[a]	$\Delta G_{\mathrm{solv}}(trans1)$	$\Delta G_{\mathrm{solv}}(\mathrm{X})$	$\Delta\Delta G_{\mathrm{solv}}(trans1-\mathrm{X})$	$\Delta G_{\mathrm{aq}}(trans1-\mathrm{X})$
B3LYP/6–31G(*d*)[b]	*trans*2	0.78	−12.12	−8.64	3.48	−2.70
	*cis*1	−2.11		−10.89	−1.23	−3.33
	*cis*2	−2.24		−9.92	−2.20	−4.44
	*cis*3	−1.82		−13.87	1.75	−0.08
B3LYP/6–31+G(*d,p*)[b]	*trans*2	−2.40	−14.23	−10.64	−3.59	−5.99
	*cis*1	−3.40		−12.78	−1.45	−4.85
	*cis*2	−4.49		−11.41	−2.82	−7.31
	*cis*3	−2.74		−15.31	1.08	−1.66
B3LYP/6–31G(2*df,p*)[c]	*trans*2	−0.44	−11.41	−7.26	−4.15	−4.60
	*cis*1	−2.62		−9.53	−1.88	−4.50
	*cis*2	−3.62		−9.24	−2.17	−5.78
	*cis*3	−2.85		−13.64	2.23	−0.62
B3LYP/6–31+G(2*df,p*)[c]	*trans*2	−2.73	−13.50	−9.17	−4.33	−7.06
	*cis*1	−3.11		−11.49	−2.01	−5.12
	*cis*2	−5.95		−11.29	−2.21	−8.16
	*cis*3	−3.52		−14.92	1.42	−2.10

All energies in $\mathrm{kcal\,mol^{-1}}$.

[a] Geometry and ZPE computed at B3LYP/6–31G(*d*) level: $E_{\mathrm{ZPE}}(trans1) = 97.59\,\mathrm{kcal\,mol^{-1}}$, $E_{\mathrm{ZPE}}(\mathrm{c}trans2) = 97.45\,\mathrm{kcal\,mol^{-1}}$, $E_{\mathrm{ZPE}}(cis1) = 97.57\,\mathrm{kcal\,mol^{-1}}$, $E_{\mathrm{ZPE}}(cis2) = 97.30\,\mathrm{kcal\,mol^{-1}}$, $E_{\mathrm{ZPE}}(cis3) = 97.94\,\mathrm{kcal\,mol^{-1}}$.

[b] Pt basis: SDD.

[c] Pt basis: SDD + 3*fg*.

Table 6
trans- and *cis*-$PtCl_2(H_2O)_2$ + $8H_2O$ clusters: energy differences (including ZPE), free energies of solvation (computed by COSMO) and resulting free energy differences in aqueous solution at 0 K

Calculation	$\Delta E_0(trans - cis)$[a]	$\Delta G_{solv}(trans)$	$\Delta G_{solv}(cis)$	$\Delta\Delta G_{solv}(trans - cis)$	$\Delta G_{aq}(trans - cis)$
B3LYP/6–31G(*d*)[b]	−3.30	−4.53	−8.13	3.60	0.30
B3LYP/6–31+G(*d,p*)[b]	0.82	−5.50	−9.34	3.84	4.66
B3LYP/6–31G(2*df,p*)[c]	−2.65	−2.14	−5.81	3.66	1.02
B3LYP/6–31+G(2*df,p*)[c]	0.60	−3.54	−7.44	3.90	4.49

All energies in kcal mol^{-1}.
[a] Geometry and ZPE computed at B3LYP/6–31G(*d*) level: $E_{ZPE}(trans) = 163.10$ kcal mol^{-1}, $E_{ZPE}(cis) = 162.46$ kcal mol^{-1}.
[b] Pt basis: SDD.
[c] Pt basis: SDD + 3*fg*.

marked fluctuation. Nevertheless, what emerges is that in solution *trans*1 and *cis*3 are consistently predicted as the lowest energy structures. The corresponding *trans* − *cis* free energy differences at 0 K range from −2.1 to −0.1 kcal mol^{-1}, which are very close to the values in Table 2.

The best estimate of the *trans* − *cis* free energy differences at 0 K, on the basis of our most extensive, viz. B3LYP/6–31+G(2*df,p*) calculations on the $PtCl_2(H_2O)_2$ + $4H_2O$ clusters is −2.1 kcal mol^{-1}. As for $PtCl_2(H_2O)_2$ itself, a correction of 0.31 kcal mol^{-1} for spin-orbit coupling and core-valence polarization [60] would 0be justified, which results in a *trans* − *cis* free energy differences at 0 K of −1.8 kcal mol^{-1}. A more contentious issue is whether, in the calculation of this quantity at 298 K, it would be justifiable to apply a thermal correction to the free energy which is computed for the gas-phase clusters, utilizing in particular their harmonic frequencies. Given that the contribution of a vibrational mode to the molecular entropy is inversely related to its frequency, low frequency intermolecular torsional and librational modes have a significant effect on the entropy. Yet these are the modes which would be most affected by the presence of solvent, i.e. interactions with further solvating molecules. We feel that the calculation of molecular entropy of a species in solution which utilizes gas-phase cluster frequencies is an unsafe and ultimately unjustifiable approach. In the context of this work, in the absence of experimental data, the importance of thermal corrections in the calculation of the *trans* − *cis* free energy difference is probably best estimated on the basis of gas-phase calculations for $PtCl_2(H_2O)_2$, which is just 0.26 kcal mol^{-1}. This is negligible really, given other, more significant potential errors in our computations, such as convergence with respect to methodology and basis set and the effect of solvent on the structure of the discrete solvation shell. Based on these calculations and the above arguments, an estimate of −1.5 ± 1.0 kcal mol^{-1} for the *trans* − *cis* free energy difference at 298 K appears reasonable, although the experimental value of −0.1 kcal mol^{-1} lies just outside the estimated error range.

The results for the clusters with eight solvating water molecules are less satisfactory. Only one structure for each isomer was considered, as shown in Figs. 4 and 5. As for the smaller systems, the geometries of these eight-water clusters were optimized at the B3LYP/6–31G(*d*) level. The variation of relative energies, both gas-phase and in solution, show a degree of variation which is similar to what had been noted for the four-water clusters. The solvation energies, in absolute terms, are over a factor of two smaller than for the four-water clusters, which make their fluctuation of ~60% that much more noticeable. The *trans* − *cis* free energy differences in aqueous solution (at 0 K) range from 0.3 to 4.5 kcal mol^{-1}, i.e. suggesting that the *cis* isomer would be the more stable isomer in solution.

As a further aid to our analysis, we estimate the *total* solvation energies of *cis*- and *trans*-$PtCl_2(H_2O)_2$ on the basis of the four- and eight-water cluster calculations, i.e. where the interactions with the discrete water molecules in the solvation shells are incorporated into the total solvation energy. Noting that the solvation process for a solute X in water is defined as

$$X + (H_2O)_\infty \rightarrow X(H_2O)_\infty \tag{1}$$

where $(H_2O)_\infty$, representing liquid water, is defined as a “cluster” of an infinite number of water molecules, the solvation energy of X, viz. reaction energy of reaction (1), is the difference in total energies

$$\Delta E_{solv} = \Delta E_\infty = E[X(H_2O)_\infty] - E[X] - E[(H_2O)_\infty], \tag{2}$$

which in turn are approximated as

$$E[X(H_2O)_\infty] = E[X(H_2O)n] + \Delta G_{solv}[X(H_2O)n] \tag{3}$$

$$E[(H_2O)_\infty] = E[(H_2O)n] + \Delta G_{solv}[(H_2O)n] \tag{4}$$

$E[X(H_2O)_n]$ and $E[(H_2O)_n]$, for $n = 4$ and 8, are the computed gas-phase energies of the four- and eight-H_2O clusters of $PtCl_2(H_2O)_2$, and of analogous $(H_2O)_4$ and $(H_2O)_8$ water clusters respectively. $\Delta G_{solv}[X(H_2O)_n]$ and $\Delta G_{solv}[(H_2O)_n]$ represent the solvation energies of the appropriate clusters, as computed by COSMO in this work. In addition to the quantities already calculated, the analogous energies for $(H_2O)_4$ and $(H_2O)_8$ needed to be computed. Starting with the cyclic and cube-like optimized Hartree–Fock structures of Maheshwary et al. [73], they were re-optimized at the B3LYP/6–31G(*d*) level, followed

Table 7
Computed solvation energies of *trans*-$PtCl_2(H_2O)_2$

	Calculation	
	n	$-\Delta E_{\mathrm{solv}}$
B3LYP/6–31G(*d*)[a]	0	22.68
	4	30.98
	8	21.56
B3LYP/6–31+G(*d,p*)[a]	0	22.63
	4	25.17
	8	15.16
B3LYP/6–31G(2*df,p*)[b]	0	21.96
	4	32.59
	8	24.33
B3LYP/6–31+G(2*df,p*)[b]	0	22.15
	4	23.52
	8	13.62

[a] Pt basis: SDD.
[b] Pt basis: SDD + 3*fg*.

by the computation of zero point energies and single point energies with the larger basis sets, as for the hydrated clusters of the platinum complexes.

The computed solvation energies for *trans*-$PtCl_2(H_2O)_2$ are given in Table 7, along with the solvation energies obtained by COSMO alone, viz. $n = 0$, from Table 2. The solvation energies deduced from the $n = 4$ and 8 calculations vary considerably with basis, but as the basis set is enlarged, especially by the addition of diffuse functions on the ligands and solvating water molecules, a reasonable degree of convergence is observed. Moreover, the solvation energy obtained from four-H_2O cluster data computed with the largest basis, viz. 23.5 kcal mol^{-1}, is consistent with the "pure continuum" value of 22.2 kcal mol^{-1}. However, the solvation energies deduced from the eight-H_2O cluster data are lower, by ∼10 kcal mol^{-1}. A plausible explanation for such an inconsistency is that a gas-phase optimized eight-H_2O cluster is not a realistic structure for solvated $PtCl_2(H_2O)_2$. Examination of the energetics shows that in solution the energy for the reaction

$$[PtCl_2(H_2O)_2 + 4H_2O] + [(H_2O)_4 \rightarrow [PtCl_2(H_2O)_2 + 8H_2O] \qquad (5)$$

is 9.1 kcal mol^{-1} at the B3LYP/6–31+G(2*df,p*) level. In other words, the addition of four extra molecules to the four-H_2O cluster is an energetically unfavourable, endothermic process. Consequently, the structures of eight-H_2O clusters in solution will be dictated as much by solvent–solvent as by solute–solvent interactions. Given these findings we propose that the eight-H_2O cluster results not be used to estimate the *trans* − *cis* solvation energy difference.

In light of the results presented in this section, we feel that the combination of discrete and continuum solvation methods, where the solvation of gas-phase optimized clusters is obtained by dielectric continuum methods, is a reasonable and workable compromise between the two limiting cases, i.e. the discrete and continuum approaches, but it needs to be applied with caution. Optimizing the cluster geometries in the presence of the solvent, viz. dielectric, may overcome the problems encountered here. (Unfortunately, due to numerical problems, such an approach did not work satisfactorily for the systems studied here.) Alternatively, a possible solution may be to work with even larger clusters, so that the structure of the first few solvation shells around a solute, such as a transition metal complex, is reasonably well described.

7. Conclusion

Describing the properties and energetics of a transition metal complex in solution is a challenging task. Nevertheless, it appears that even with formally simple and fast methods, like DFT, coupled with a PCM model of solvation such as COSMO, reasonable results can be obtained. This work concentrated on the description of the $PtCl_2(H_2O)_2$ complex, in particular on the reliable computation of the *trans* − *cis* free energy difference (ΔG^0) in gas-phase and in aqueous solution. At 0 K, based on coupled cluster calculations, our best estimate of this quantity in the gas phase is 0.1 kcal mol^{-1}. The analogous value at 298 K in aqueous solution, based on DFT and COSMO calculations, is −0.8 kcal mol^{-1}, which is in good agreement with the experimental value of −0.1 kcal mol^{-1}. Moreover, as these relative energies are quite stable with respect to basis set variation, results of acceptable accuracy were obtained with modest bases of 6–31G(*d*) quality.

Application of the EFP method in conjunction with the HF formalism yielded values ranging approximately from −12 to 2 kcal mol^{-1}, depending on the sizes and structures of the clusters. Such scatter, reflecting the sensitivity of the energies to the choice of clusters is the most serious problem of such calculations, especially as the cluster becomes larger.

The hybrid approach, where a dielectric continuum method is used in combination with cluster calculations, was explored, where four and eight solvating molecules were explicitly included in the DFT supermolecule calculations. On the basis of four-H_2O solvated cluster computations we obtained a value of -1.5 ± 1.0 kcal mol^{-1} as the *trans* − *cis* free energy difference, in good agreement, again, with experiment. As these calculations require an accurate quantum chemical description of hydrogen bonded clusters, the basis set requirements are considerably more stringent than for the application of a continuum method. Analogous calculations on eight-H_2O clusters revealed a potential problem with such an approach, whereby the gas-phase determination of the solvated structure may not be realistic, as it ignores the effect of the interactions with the bulk solvent.

It is gratifying that with respect to the computation of *trans* − *cis* energy difference a good level of agreement with experiment, within approximately 1 kcal mol^{-1}, can be achieved by the application of DFT coupled with COSMO.

The consistency of the solvation energies, when comparing the most reliable estimate from the four-H_2O cluster calculation with the prediction by COSMO, suggests that the above success of the methods is due more to the accuracy of the computed solvation energies than fortuitous cancellations.

These calculations provide a convenient benchmark for estimation of the reliability of a calculation of equilibrium solvation effects in transition metal complexes and, and by extension of solvation along a reaction pathway. Our experience with cluster models should be helpful in the design of similar models for both complexes and free ligands.

Acknowledgements

We wish to express our thanks to the Australian Partnership for Advanced Computing National Facility for access to the COMPAQ AlphaServer SC system. This work was supported by the Australian Research Council.

References

[1] J.S. Craw, G.B. Bacskay, N.S. Hush, Inorg. Chem. 32 (1993) 2230.
[2] J.S. Craw, G.B. Bacskay, N.S. Hush, J. Am. Chem. Soc. 116 (1994) 5937.
[3] I. Bytheway, G.B. Bacskay, N.S. Hush, J. Phys. Chem. 100 (1996) 6023.
[4] I. Bytheway, G.B. Bacskay, N.S. Hush, J. Am. Chem. Soc. 118 (1996) 3753.
[5] N.S. Hush, J. Am. Chem. Soc. 119 (1997) 1717.
[6] I. Bytheway, J.S. Craw, G.B. Bacskay, N.S. Hush, in: S.S. Isied (Ed.), Taube Insights: From Electron Transfer Reactions to Modern Inorganic Chemistry, Advances in Chemistry Series, vol. 253, American Chemical Society, Washington, DC, 1997, p. 21.
[7] I. Bytheway, G.B. Bacskay, N.S. Hush, J. Phys. Chem. 100 (1996) 14899.
[8] K. Mylvaganam, G.B. Bacskay, N.S. Hush, J. Am. Chem. Soc. 123 (2001) 5495.
[9] R.A. Periana, D.J. Taube, S. Gamble, H. Taube, T. Satoh, H. Fuji, Science 280 (1998) 560.
[10] K. Mylvaganam, G.B. Bacskay, N.S. Hush, J. Am. Chem. Soc. 121 (1999) 4633.
[11] K. Mylvaganam, G.B. Bacskay, N.S. Hush, J. Am. Chem. Soc. 122 (2000) 2041.
[12] J. Zeng, J.S. Craw, N.S. Hush, J.R. Reimers, Chem. Phys. Lett. 206 (1993) 323.
[13] J. Zeng, C. Woywod, J.S. Craw, N.S. Hush, J.R. Reimers, J. Am. Chem. Soc. 117 (1995) 8618.
[14] J. Zeng, J.S. Craw, N.S. Hush, J.R. Reimers, J. Chem. Phys. 99 (1993) 1482.
[15] J. Zeng, N.S. Hush, J.R. Reimers, J. Chem. Phys. 99 (1993) 1496.
[16] J. Zeng, N.S. Hush, J.R. Reimers, J. Chem. Phys. 99 (1993) 1508.
[17] J. Zeng, N.S. Hush, J.R. Reimers, J. Chem. Phys. 100 (1996) 9561.
[18] J. Zeng, N.S. Hush, J.R. Reimers, J. Phys. Chem. 99 (1995) 10459.
[19] J. Zeng, N.S. Hush, J.R. Reimers, J. Phys. Chem. 100 (1996) 19292.
[20] J. Zeng, N.S. Hush, J.R. Reimers, J. Am. Chem. Soc. 118 (1996) 2059.
[21] J. Zeng, J.S. Craw, N.S. Hush, J.R. Reimers, J. Phys. Chem. 98 (1994) 11075.
[22] N.S. Hush, J. Zeng, J.R. Reimers, J.S. Craw, Adv. Chem. Ser. Photochem. Radiat. Chem. 254 (1998) 263.
[23] N.S. Hush, J.R. Reimers, Coord. Chem. Rev. 177 (1998) 37.
[24] N.S. Hush, J.R. Reimers, Chem. Rev. 100 (2000) 775.
[25] L.I. Elding, Acta Chem. Scand. 24 (1970) 1331.
[26] L.I. Elding, Acta Chem. Scand. 24 (1970) 1341.
[27] O. Gröning, L.I. Elding, Inorg. Chem. 28 (1989) 3366.
[28] P.E.M. Siegbahn, R.H. Crabtree, Mol. Phys. 89 (1996) 279.
[29] G. B. Bacskay, J. R. Reimers, in: P.V.R. Schleyer (Ed.), Encyclopedia of Computational Chemistry, J. Wiley and Sons, Chichester, 1998, p. 2620.
[30] P. Bandyopadhyay, M.S. Gordon, J. Chem. Phys. 113 (2000) 1104.
[31] J.H. Jensen, P.N. Day, M.S. Gordon, H. Basch, D. Cohen, D.R. Garmer, M. Krauss, W. J. Stevens, in: D.A. Smith (Ed.), Modeling the Hydrogen Bond, ACS Symposium Series, vol. 569, American Chemical Society, Washington, DC, 1994, p. 139.
[32] P.N. Day, J.H. Jensen, M.S. Gordon, S.P. Webb, W.J. Stevens, M. Krauss, D. Garmer, H. Basch, D.J. Cohen, Chem. Phys. 105 (1996) 1968.
[33] W. Chen, M.S. Gordon, J. Chem. Phys. 107 (1997) 11081.
[34] M. Krauss, S.P. Webb, J. Chem. Phys. 107 (1997) 5771.
[35] P.N. Day, R. Pachter, J. Chem. Phys. 107 (1997) 2990.
[36] M.S. Gordon, M.A. Freitag, P. Bandyopadhyay, V. Kairys, J.H. Jensen, W.J. Stevens, J. Phys. Chem. A 105 (2001) 293.
[37] I. Adamovic, M.A. Freitag, M.S. Gordon, J. Chem. Phys. 118 (2003) 6725.
[38] G.N. Merrill, M.S. Gordon, J. Phys. Chem. A 102 (1998) 2650.
[39] P. Bandyopadhyay, B. Mennucci, J. Tomasi, M.S. Gordon, J. Chem. Phys. 116 (2002) 5023.
[40] P.C. Petersen, M.S. Gordon, J. Phys. Chem. A 103 (1999) 4162.
[41] M.A. Freitag, M.S. Gordon, Book of Abstracts, 218th ACS National Meeting, New Orleans, 22–26 August 1999, COMP-114.
[42] A. Yoshikawa, M.S. Gordon, Book of Abstracts, 218th ACS National Meeting, New Orleans, 22–26 August 1999, PHYS-281.
[43] M. Krauss, S.P. Webb, J. Chem. Phys. 107 (1997) 5771.
[44] S.E. Worthington, M. Krauss, Comput. Chem. 24 (2000) 275, and references therein.
[45] A. Klamt, G.J. Schüürmann, J. Chem. Soc., Perkin Trans. 2 (1993) 799.
[46] A. Klamt, J. Phys. Chem. 99 (1995) 2224.
[47] A. Klamt, V.J. Jonas, Chem. Phys. 105 (1996) 9972.
[48] C. Lee, W. Yang, R.G. Parr, Phys. Rev. B 37 (1988) 385.
[49] A.D. Becke, J. Chem. Phys. 98 (1993) 5648.
[50] K. Raghavachari, G.W. Trucks, J.A. Pople, M. Head-Gordon, Chem. Phys. Lett. 157 (1989) 479.
[51] D. Andrae, U. Häussermann, M. Dolg, H. Stoll, H. Preuss, Theor. Chem. Acta 77 (1990) 123.
[52] S. Huzinaga, J. Chem. Phys. 42 (1965) 1293.
[53] W.J. Stevens, H. Basch, M. Krauss, J. Chem. Phys. 81 (1984) 6026.
[54] W.J. Stevens, M. Krauss, H. Basch, P.G. Jasien, Can. J. Chem. 70 (1992) 612.
[55] T.R. Cundari, W.J. Stevens, J. Chem. Phys. 98 (1993) 5555.
[56] M.W. Schmidt, K.K. Baldridge, J.A. Boatz, S.T. Elbert, M.S. Gordon, J.H. Jensen, S. Koseki, N. Matsunaga, K.A. Nguyen, S. Su, T.L. Windus, M. Dupuis, J.A. Montgomery, J. Comput. Chem. 14 (1993) 1347.
[57] M.J. Frisch, G.W. Trucks, H.B. Schlegel, G.E. Scuseria, M.A. Robb, J.R. Cheeseman, V.G. Zakrzewski, J.A. Montgomery Jr., R.E. Stratmann, J.C. Burant, S. Dapprich, J.M. Millam, A.D. Daniels, K.N. Kudin, M.C. Strain, O. Farkas, J. Tomasi, V. Barone, M. Cossi, R. Cammi, B. Mennucci, C. Pomelli, C. Adamo, S. Clifford, J. Ochterski, G.A. Petersson, P.Y. Ayala, Q. Cui, K. Morokuma, D.K. Malick, A.D. Rabuck, K. Raghavachari, J.B. Foresman, J. Cioslowski, J.V. Ortiz, A.G. Baboul, B.B. Stefanov, G. Liu, A. Liashenko, P. Piskorz, I. Komaromi, R. Gomperts, R.L. Martin, D.J. Fox, T. Keith, M.A. Al-Laham, C.Y. Peng, A. Nanayakkara, C. Gonzalez, M. Challacombe, P.M.W. Gill, B. Johnson, W. Chen, M.W. Wong, J.L. Andres, C. Gonzalez, M. Head-Gordon, E.S. Replogle, J.A. Pople, Gaussian 98, Revision A.7, Gaussian Inc., Pittsburgh, PA, 1998.

[58] M.J. Frisch, G.W. Trucks, H.B. Schlegel, G.E. Scuseria, M.A. Robb, J.R. Cheeseman, J.A. Montgomery Jr., T. Vreven, K.N. Kudin, J.C. Burant, J.M. Millam, S.S. Iyengar, J. Tomasi, V. Barone, B. Mennucci, M. Cossi, G. Scalmani, N. Rega, G.A. Petersson, H. Nakatsuji, M. Hada, M. Ehara, K. Toyota, R. Fukuda, J. Hasegawa, M. Ishida, T. Nakajima, Y. Honda, O. Kitao, H. Nakai, M. Klene, X. Li, J.E. Knox, H.P. Hratchian, J.B. Cross, C. Adamo, J. Jaramillo, R. Gomperts, R.E. Stratmann, O. Yazyev, A.J. Austin, R. Cammi, C. Pomelli, J.W. Ochterski, P.Y. Ayala, K. Morokuma, G.A. Voth, P. Salvador, J.J. Dannenberg, V.G. Zakrzewski, S. Dapprich, A.D. Daniels, M.C. Strain, O. Farkas, D.K. Malick, A.D. Rabuck, K. Raghavachari, J.B. Foresman, J.V. Ortiz, Q. Cui, A.G. Baboul, S. Clifford, J. Cioslowski, B.B. Stefanov, G. Liu, A. Liashenko, P. Piskorz, I. Komaromi, R.L. Martin, D.J. Fox, T. Keith, M.A. Al-Laham, C.Y. Peng, A. Nanayakkara, M. Challacombe, P.M.W. Gill, B. Johnson, W. Chen, M.W. Wong, C. Gonzalez, J.A. Pople, Gaussian 03, Revision B.03, Gaussian Inc., Pittsburgh, PA, 2003.

[59] T.G. Appleton, H.C. Clark, L.E. Manzer, Coord. Chem. Rev. 10 (1973) 335.

[60] J.V. Burda, M. Zeizinger, J. Šponer, J. Leszczynski, J. Chem. Phys. 113 (2000) 2224.

[61] E.R. Davidson, J. Chem. Phys. 46 (1967) 3320.

[62] K.R. Roby, Mol. Phys. 27 (1974) 81.

[63] R. Heinzmann, R. Ahlrichs, Theor. Chim. Acta 42 (1976) 33.

[64] C. Ehrhardt, R. Ahlrichs, Theor. Chim. Acta 68 (1985) 231.

[65] J.P. Foster, F. Weinhold, J. Am. Chem. Soc. 102 (1980) 7211.

[66] A.E. Reed, F. Weinhold, J. Chem. Phys. 78 (1983) 4066.

[67] A.E. Reed, R.B. Weinstock, F. Weinhold, J. Chem. Phys. 83 (1985) 735.

[68] T.-X. Lü, G.B. Bacskay, A.D.J. Haymet, Mol. Phys. 88 (1996) 173.

[69] J. Tomasi, M. Persico, Chem. Rev. 94 (1994) 2027.

[70] HyperChem Release 5.0 for Windows, Hypercube Inc., Waterloo, Ontario, Canada, 1996.

[71] H.M. Netzloff, M.S. Gordon, J. Sorenson, M. Grant, Book of Abstracts, 222nd ACS National Meeting, Chicago, 26–30 August 2001, PHYS-293.

[72] H.M. Netzloff, M.S. Gordon, J. Sorenson, Book of Abstracts, 223rd ACS National Meeting, Orlando, 7–11 April 2002, COMP-169.

[73] S. Maheshwary, N. Patel, N. Sathyamurthy, A.D. Kulkarni, S.R. Gadre, J. Phys. Chem. A 105 (2001) 10525.